NANO LETTERS

XXXX
Vol. xx, No. x
000-

Distance Dependent Spectral Tuning of Two Coupled Metal Nanoparticles

Phillip Olk,*,† Jan Renger,‡ Marc Tobias Wenzel,† and Lukas M. Eng†

Institut für Angewandte Photophysik, TU Dresden, 01062 Dresden, Germany, and ICFO-Institut de Ciencies Fotoniques, Mediterranean Technology Park, 08860 Castelldefels, Barcelona, Spain

Received January 7, 2008; Revised Manuscript Received February 25, 2008

ABSTRACT

The spectral properties of two spherical metallic nanoparticles of 80 nm in diameter are examined with regard to the interparticle distance and relative polarization of the excitation light. One Au nanoparticle is attached to a scanning fiber probe and the second to a scanning substrate. This configuration allows three-dimensional and arbitrary manipulation of both distance and relative orientation with respect to the incident light polarization. As supported by numerical simulations, a periodic modulation of the coupled plasmon resonance is observed for separations smaller than 1.5 μm. This interparticle coupling affects the scattering cross section in terms of spectral position and spectral width as well as the integral intensity of the Mie-scattered light.

Spherical metal nanoparticles (MNPs) and their plasmon resonances are well-known as guinea pigs for their optical properties,[1] particularly when examining optical near-fields.[2] For instance, substrates partly covered with MNPs are intensively used for surface-enhanced fluorescence and Raman scattering experiments.[3] If attached to a scanning probe tip, a *single* MNP can be ideally used as a well-confined scattering object for instance in (scattering) scanning near-field optical microscopy (SNOM).[4–7] The plasmon resonance of such an isolated MNP interacting with its environment was used for scanning probe fluorescence microscopy,[8,9] scanning particle radiation spectroscopy,[10] and scanning particle enhanced Raman microscopy.[11]

Placing *two* MNPs a short distance apart from each other is of particular interest as the plasmons of the individual MNPs couple.[12] Because of this coupling, the expected field enhancement of such "dimers" easily exceeds the single particle response for resonant excitation.[13,14] This may produce, e.g., high Raman signals.[11,13,15,16] In such a two-MNP setup, two cases, A and B, as schematically depicted in Figure 1 (left), may be considered:

Case A: For an illuminating beam polarized *parallel* to the principal axis (i.e., along the line connecting the centers of the two MNPs), the two particles interact by means of near-field coupling.[17–19] As a rule of thumb, the two particles strongly couple if they are separated less than the particle diameter.[20] The near-field coupling manifests in a strong field enhancement between the two MNPs.[11,16] Additionally, it was shown[12,21] that the two individual plasmon resonances of the MNPs couple to an effective and red-shifted resonance. The precise spectral properties of the overall plasmon resonance of two coupled MNPs are subject to their material, shape, size, orientation, distance, and surrounding medium.[12,22–26]

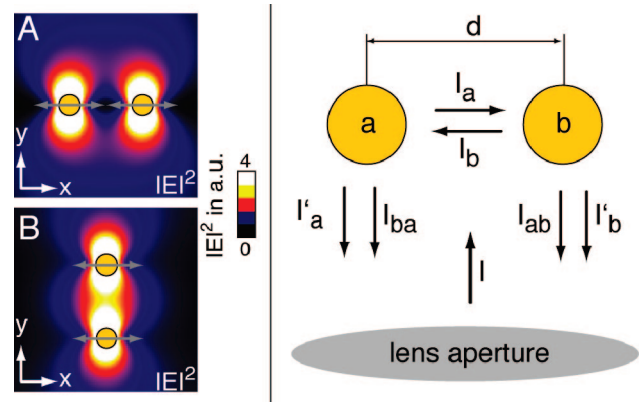

Figure 1. (left) Sketch of the $\cos^2\theta$-dependent far-field intensity distribution of two point dipoles[34] separated by 10λ, illustrating two relative orientations. (A) The incident polarization is parallel to the principal axis connecting the two particles. The induced dipoles (depicted by the gray arrows) are collinear, hence no far-field coupling is possible. (B) The relative orientation of the induced dipoles allows for far-field coupling. (right) Illustration of occurring intensity components: the illumination I is scattered by particles a and b. Portions of the scattered light I_a and I_b may be scattered again by the opposite particles b or a and then caught by the microscope lens as I_{ba} and I_{ab}. Behind the lens, the originally scattered light I'_a and I'_b may interfere with I_{ba} and I_{ab} at the spectrometer slit. The relative phase shift between the I'_n and the I_{nm} is dependent on the distance d.

* Corresponding author. E-mail: polk@iapp.de. Web site: http://iapp.de.
† Institut für Angewandte Photophysik, TU Dresden.
‡ ICFO-Institut de Ciencies Fotoniques.

10.1021/nl080044m CCC: $40.75
Published on Web 03/14/2008

Case B: For an illumination polarized *perpendicularly* to the principal axis, the near-field coupling of the two particles is very weak,[22,26] as the surface-adjacent regions of high near-fields are pointing away from the neighboring MNP. Alas, the orientation of the induced dipoles facilitates *far-field* interaction of the MNPs, as the two MNPs are located in the dipolar emission field of its neighboring particle. Taking retardation effects into full account, a distance-dependent oscillation of the two-particle plasmon energy and plasmon line width is expected.[22] For that case, an overall blue-shift of the extinction spectrum was already reported for small particle separations.[21]

In this Letter, we experimentally and theoretically examine the distance dependence of the spectral scattering cross section (SCS) of such a system consisting of two 80 nm gold spheres separated at a variable distance d embedded in a medium of refractive index $n = 1.52$. The spectral position and the spectral line width of the back-scattered light will be shown to be modulated. To substantiate this expectation, we perform numerical calculations by means of the multiple multipole technique.[27–29] The model used here uses plane waves as the illumination,[22] but it takes into account that the SCS is measured in back-scattering configuration using a lens of finite numerical aperture.

In our experimental approach, we attach one gold nanoparticle of 80 nm in diameter to the apex of a tapered optical fiber, the latter serving as a single particle manipulator, following an established procedure.[4,11] The fiber is then mounted on a quartz tuning fork, which serves as a distance-sensitive feedback control similar to SNOM.[30] Because both particles are immersed in an index matching oil ($n = 1.52$), unwanted reflections from the substrate's surface are suppressed. Furthermore, the submerged fiber tip nearly vanishes optically, thus serving only as a position-sensitive manipulator for the adherent gold particle; the fiber is not used here for any optical purpose.

The optical quality of all MNPs utilized here is verified by recording their back-scattering spectra:[31] the *spectral position* of the back-scattered light provides information on the size of the particle, while the *overall intensity* of the (back-)scattered light ensures that only one particle is examined, and the *shape* of the spectra verifies the spherical property of the particle under examination.

A sketch of the experimental setup is depicted in Figure 2. The tip particle, a, is positioned in the center of the illumination field of a 100× micoscope lens (Zeiss Plan-Neofluar, N.A. = 1.3), which is mounted on an inverted optical microscope (Zeiss Axiovert 200). This particle is kept at its designated lateral and vertical position using a shear−force feedback loop for controlling the tip−subtrate distance.

The illumination is provided by a 150 W Xe arc lamp covering the whole visible spectrum. Its collimated light is polarized by means of a Glan−Thompson prism, properly diverged and imaged through the microscope lens on the object plane, resulting in a circle of 5 μm radius with uniform intensity and a low divergence angle of $<10°$. Despite of the large numerical aperture, the illumination is a reasonable

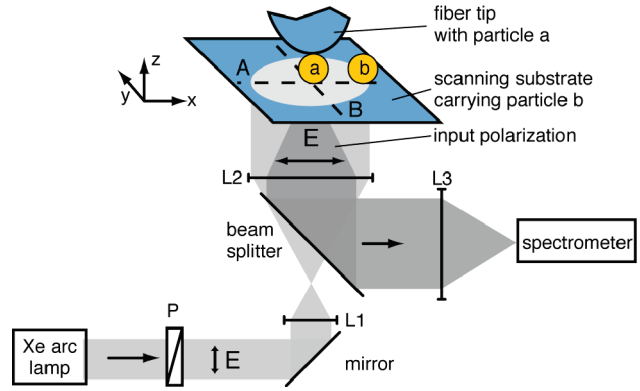

Figure 2. Cartoon of the setup. One MNP (a) is manipulated by a fiber tip, while the second MNP (b) is positioned by moving the glass substrate. While MNP (a) is kept always in the center of a white light beam (light gray circle), MNP (b) is moved along the dashed lines A and B. The collimated light of a Xe white light lamp (light gray) passes polarizer P and lens L1 and is recollimated by the microscope lens L2. The back-scattered light (dark gray) is collected by L2 and focused by L3 on the entrance slit of a spectrometer.

implementation of a plane wave excitation. Therefore, contributions from out-of-plane components of the electric field are negligible. The microscope lens design demands an immersion liquid between lens and substrate, so the substrate is sandwiched between two layers of immersion oil. Both layers improve the signal-to-noise ratio of the spectrometer by lowering the background light, as reflections of the illumination caused by the substrate interface are suppressed. Any back-scattered light is collected by the microscope lens and deflected on the entrance slit of the spectrometer.

To examine the near- and far-field interactions of the tip with a second MNP (b), additional 80 nm MNPs were dispersed on the glass substrate (BK7 cover slide) with a lateral spacing of >10 μm. According to the aforementioned criteria for particle size and shape, individual MNPs were then selected and moved into the center of the illumination spot by means of a piezoelectric translation stage, to which the glass slide was mounted. Confocal scanning of the substrate (with the tip being retracted) proved that only one particle was positioned within the illumination field and could be detected by the spectrometer.

Now, the substrate carrying the second particle (b) is scanned under the reapproached particle tip, and a full spectrum of the back-scattered light is taken at every image pixel. The relative position of the two particles can be deduced from the topography signal: particle (a) is kept at a fixed position by means of a fiber probe. If the scanned MNP (b) touches the tip-adherent MNP (a), the shear-force controller retracts the tip; this provides the absolute position of two touching MNP (center−center distance $d = 80$ nm). As the substrate carrying MNP (b) is scanned by a gauged translation stage (Piezosystem Jena, position accuracy <2 nm), the relative distance of the two MNP can be metered directly by monitoring the translation stage position.

To keep the amount of the collected data reasonable, a pixel distance of 15 nm was chosen, as this spatial sampling

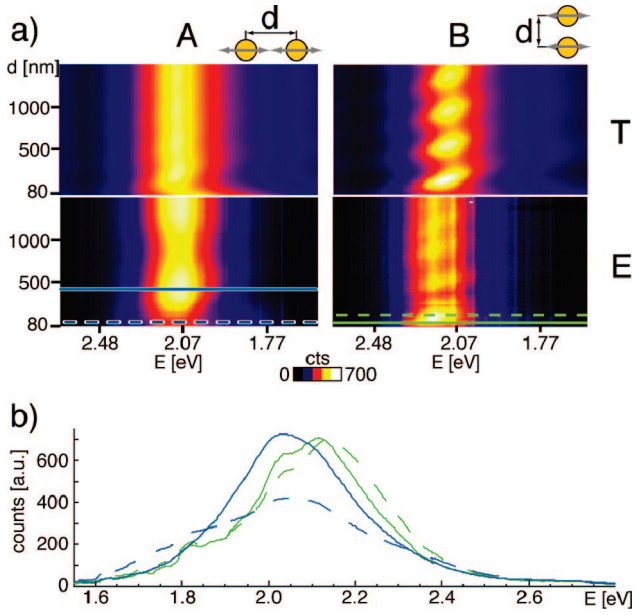

Figure 3. (a) Optical spectra both calculated (upper row) and experimentally recorded (lower row) for cases A (left) and B (right). In case B, a d-dependent modulation can be identified. The measured spectra are slightly shifted with respect to the simulation due to the actual size of the two MNPs.[31] (b) Measured spectra, line sections from (a). Converted to energy presentation for convenience. In case A (blue), the curves correspond either to spectra of far-field dominated distances of $\approx$ 400 nm (solid line) or for $d = 95$ nm. A spectral broadening and a red-shifted center position can be identified. For case B (green curves), two curves of identical height but different centers are chosen ($d = 120$ nm (solid) and $d = 200$ nm (dashed)).

rate is high enough for detecting the spectral modulation, which is the main subject of this Letter. A detailed review of the implications of the "last nanometers" and an accurate examination of nearly touching particles cannot be provided by this set of parameters and will be presented elsewhere.

In Figure 3, exemplary results are shown for two sections along lines corresponding to the cases A and B in Figures 1 and 2.

For every distance-related spectrum in Figure 3, the spectral key properties are determined, consisting of the maximum's position E_0 and the spectral width using FWHM. This is done repeatedly for three particle pairs for every orientation A and B, as in Figure 1.

For each configuration A or B, the distance-dependent fit parameters FWHM and E_0, averaged over three different MNP pairs, are plotted in Figure 4. Several key features can be found in our calculations and measurements (Figure 3), and in the appendant parameters FWHM and E_0 (Figure 4):

For large interparticle distances, $d > 1$ μm, the magnitude of the modulation depth decreases and is dominated by the apparatus drift. This applies for both cases A and B. Especially the near-field moderated coupling influence on FWHM and E_0 (case A) vanishes on a scale of $\approx$600 nm, corresponding to the wavelength of visible light. Therefore, we deduce from Figure 3 (solid blue curves) and Figure 4 that for arrangement A, no significant interaction takes place between the two particles at larger separations.

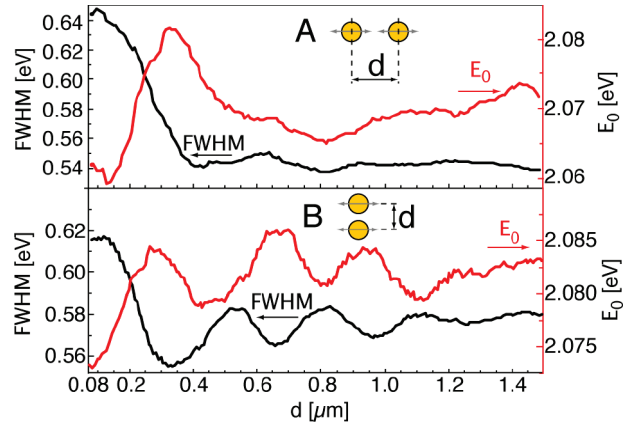

Figure 4. Plots of the spectral properties (FWHM and center energy E_0) of the light back-scattered by two coupling MNPs with variable interparticle distance d. Whereas for case A, only near-field mediated coupling for $d < \lambda$ occurs, case B shows a modulation of the spectral features that is caused by far-field effects.

For smaller distances, the two adjacent MNPs couple and therefore change their spectral properties (Figure 3, dashed blue curve); while the scattering intensity at the individual particle resonance ($\approx$2.08 eV) is reduced by about 30%, the SCS increases in the spectral range below $\sim$1.85 eV. Effectively, this leads to an increase of the overall FWHM.

For a polarization as depicted in case B, the spectral FWHM shows a very similar behavior as for case A provided the two spheres are very close, i.e., $d < 200$ nm (Figure 3, solid green curve). Additionally, a far-field coupling leads to a modulation of the spectral properties, with a periodicity of $\approx$350 nm. According to Figure 1 (right), this spatial periodicity can be assigned to the phase relation between different components of the detected light: the interference of light directly scattered by a selected MNP (e.g., I_a' scattered by MNP (a)), and light that was scattered by the other particle (b) and then rescattered by the first one (I_{ab}). As depicted in Figure 1, this mechanism works for both directions, i.e., directly back-scattered light from MNP (b) interferes with light rescattered via (a) and (b).

Bearing in mind that the illumination consists of a continuous spectrum, any distance-related phase shift will produce constructive interference for at least one wavelength. Such a periodic modulation is found, e.g., in the context of forces between MNPs, too.[32,33] It should be noted that the resonant properties of the particles affect only the modulation *depth* and not the periodicity; the latter originates from the distance-dependent phase difference of the scattered light.

While these aspects are well documented by both experiment and calculations, three certain facets must be emphasized:

(1) From calculations,[22,31] one would expect a distinct far-field coupling for distances d even larger than 2 μm, while our measurements show such a modulation only up to $d \approx$ 1.5 μm. This is owed to the fact that the calculations assume a plane-wave excitation of infinite coherence length, whereas the used Xe arc lamp provides a bandwidth-limited coherence length of $L_c \approx 1$ μm, thus cutting off the phase-sensitive interaction between the two MNPs at larger distances.

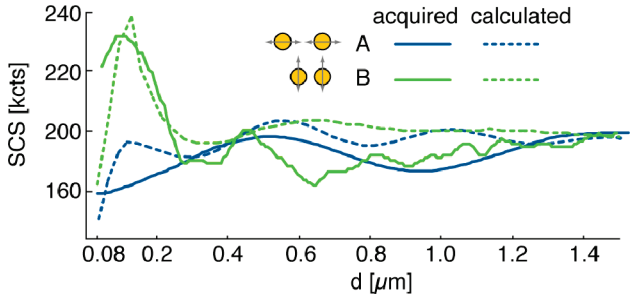

Figure 5. Integral SCS for case A (blue curves) and B (green curves), both calculated (dashed) and measured (solid, average of three data sets). While the acquired integral SCS appears to decrease by 20% for case A, case B shows a more complex behavior, which is found in our calculation as well.

(2) Because of the averaging of several data sets with different MNP diameter-related center energies E_0, the FWHM is larger than expected for a single MNP. In turn, the modulation depth is smaller than predicted.[22,31]

(3) A narrowing of the FWHM was predicted in ref 22 for very close distances (d < 100 nm). This narrowing was not observed, neither by us nor by other experiments.[21] This is *not* owed to the averaging over multiple MNP pairs. Indeed, a closer look at similar calculations[17] suggests a spectral narrowing of the resonance assigned to the single MNP, but *additionally*, a *second* resonance appears slightly red-shifted to the original peak, which may be assigned to the strongly interacting two particle system, which behaves like an elongated particle. When treating *both* contributions as one apparent peak, the overall spectral width of the SCS does not decrease, but effectively increases!

In addition to the spectral FWHM and spectral position E_0, we also recorded the integral amplitude of the SCS. For each particle distance, the area of the simulated and measured SCS was calculated. These results are shown in Figure 5.

A relative polarization according to case A leads to a *decrease* of the integral SCS for distances, allowing for near-field coupling. The coupling introduces a second, red-shifted resonance caused by the resonance splitting. This red-shift of the overall resonance reduces the integral SCS as scattering efficiencies of such small particles are proportional to $1/\lambda^4$.[34]

For alignment B, the integral SCS *increases* for distances around 150 nm. At this position, the overall spectral broadening (Figure 4) is not very prominent. For this situation, one may consider the two MNPs to enhance each other's SCS. If the two particles are approached further, the effect of near-field coupling counter-balances this antenna-like effect, whereby the integral SCS decreases again.

The comparison of our numerical simulations to the experimental data turns out to be satisfactory: for case A, the smooth trend of the decreasing SCS is rendered. As for case B, the increase of the integral SCS for d < 250 nm is concisely obtained.

In summary, this Letter experimentally and numerically verifies the distance-dependent modulations of the SCS for preselected MNP pairs. The modulation affects the spectral position of the back-scattered light, its spectral width, and the overall intensity. In a future application, these effects could be exploited in order to determine the distance of two MNPs of known diameter by white light spectroscopy, e.g., in probeless experiments[16] or in systems of mesoscopic scale, where distances already are below the diffraction limit but too large in order to utilize near-field coupling as a ruler. On the other hand, active devices are imaginable, where a change of interparticle distances switches the device's sensitivity for a certain wavelength or polarization, as for signal processing. At last, this kind of experiment enables us to gather information on more complex systems, consisting, e.g., of three and four MNP.[13]

Acknowledgment. P.O. and M.T.W. kindly appreciate funding through the Specific Target Research Project PLEAS and the Network of Excellence for Plasmo-Nano-Devices. J.R. acknowledges the Specific Target Research Project PLASMOCOM. All projects are hosted by the European Union in the Sixth Framework Programme. We thank Kerstin Knott and Horst Hartmann for hints in chemistry, Thomas Härtling for spectral knowledge, and also René Schneider for fiber craft support.

Supporting Information Available: Back-scattered light from the particles used for experiments, averaged for three sets of particles. Plot of the calculated SCS for the depicted orientations (case B). This material is available free of charge via the Internet at http://pubs.acs.org.

References

(1) Kreibig, U.; Vollmer, M. *Optical Properties of Metal Clusters*; Springer Series in Materials Science 25; Springer: Heidelberg, Germany, 1995.
(2) Novotny, L.; Hecht, B. *Principles of Nano-Optics*; Cambridge University Press: New York, 2006.
(3) Chumanov, G.; Sokolov, K.; Gregory, B. W.; Cotton, T. M. *J. Phys. Chem.* **1995**, *99*, 9466.
(4) Kalkbrenner, T.; Ramstein, M.; Mlynek, J.; Sandoghdar, V. *J. Microsc.* **2001**, *202–1*, 72.
(5) Renger, J.; Grafström, S.; Eng, L. M.; Hillenbrand, R. *Phys. Rev. B* **2005**, *71*, 75410.
(6) Schneider, S.; Seidel, J.; Grafström, S.; Eng, L. M.; Winnerl, S.; Stehr, D.; Helm, M. *Appl. Phys. Lett.* **2007**, *90*, 143101.
(7) Kim, Z. H.; Leone, S. R. *J. Phys. Chem. B* **2006**, *110*, 19804.
(8) Anger, P.; Bharadwaj, P.; Novotny, L. *Phys. Rev. Lett.* **2006**, *96*, 113002.
(9) Kühn, S.; Håkanson, U.; Rogobete, L.; Sandoghdar, V. *Phys. Rev. Lett.* **2006**, *97*, 017402.
(10) Kalkbrenner, T.; Håkanson, U.; Schädle, A.; Burger, S.; Henkel, C.; Sandoghdar, V. *Phys. Rev. Lett.* **2005**, *95*, 200801.
(11) Olk, P.; Renger, J.; Härtling, T.; Wenzel, M. T.; Eng, L. M. *Nano Lett.* **2007**, *7*, 1736.
(12) Su, K.-H.; Wei, Q.-H.; Zhang, X.; Mock, J. J.; Smith, D. R.; Schultz, S. *Nano Lett.* **2003**, *3*, 1087.
(13) Li, K.; Stockman, M. I.; Bergman, D. J. *Phys. Rev. Lett.* **2003**, *91*, 227402.
(14) Romero, I.; Aizpurua, J.; Bryant, G. W.; García de Abajo, F. J. *Opt. Express* **2006**, *14*, 9988.
(15) Talley, C. E.; Jackson, J. B.; Oubre, C.; Grady, N. K.; Hollars, C. W.; Lane, S. M.; Huser, T. R.; Nordlander, P.; Halas, N. J. *Nano Lett.* **2005**, *5*, 1569.
(16) Svedberg, F.; Li, Z.; Xu, H.; Käll, M. *Nano Lett.* **2006**, *6*, 2639.
(17) Kottmann, J.; Martin, O. *Opt. Express* **2001**, *8*, 655.
(18) Blanco, L. A.; García de Abajo, F. J. *Phys. Rev. B* **2004**, *69*, 205414.
(19) ten Bloemendal, D.; Ghenuche, P.; Quidant, R.; Cormack, I. G.; Loza-Alvarez, P.; Badenes, G. *Plasmonics* **2006**, *1*, 41.
(20) Jones, T. B. *Electromechanics of Particles*; Cambridge University Press, New York, 1995.
(21) Rechberger, W.; Hohenau, A.; Leitner, A.; Krenn, J.; Lamprecht, B.; Aussenegg, F. *Opt. Commun.* **2003**, *220*, 137.

(22) Dahmen, C.; Schmidt, B.; von Plessen, G. *Nano Lett.* **2007**, *7*, 318.
(23) Sönnichsen, C. *Plasmons in Metal Nanostructures*; Cuviller Verlag: Göttingen, 2001.
(24) Bosbach, J.; Hendrich, C.; Stietz, F.; Vartanyan, T.; Träger, F. *Phys. Rev. Lett.* **2002**, *89*, 257404.
(25) Renger, J. Excitation, Interaction, and Scattering of Localized and Propagating Surface Polaritons. Ph.D. Thesis., Technical University, Dresden, 2006.
(26) Renger, J.; Grafström, S.; Eng, L. M.; Deckert, V. *J. Opt. Soc. Am. A* **2004**, *21*, 1362.
(27) Hafner, C. *The Generalized Multipole Technique for Computational Electromagnetics*; Artech House, Norwood, MA, 1990.
(28) Hafner, C.; Bomholt, L. *The 3D Electrodynamic Wave Simulator*; Wiley: Chichester, UK, 1993.
(29) Hafner, C. *Post-Modern Electromagnetics Using Intelligent MaXwell Solvers*; Wiley: Chichester, UK, 1999.
(30) Karrai, K.; Grober, R. D. *Appl. Phys. Lett.* **1995**, *66*, 1842.
(31) See Supporting Information.
(32) Chaumet, P. C.; Nieto-Vesperinas, M. *Phys. Rev. B* **2001**, *64*, 35422.
(33) Zelenina, A. S.; Quidant, R.; Nieto-Vesperinas, M. *Opt. Lett.* **2007**, *32*, 1156.
(34) Jackson, J. D. *Classical Electrodynamics*, 3rd ed.; Wiley & Sons: New York, 1998.

NL080044M